JOURNAL OF MATERIALS SCIENCE 7 (1972) 567–576

The Role of Oxygen and Nitrogen in the Recovery Process of Niobium

MOTOKUNI ETO*
Graduate School, University of Tokyo, Tokyo, Japan

Electrical resistivity and Vickers hardness were measured in order to clarify the role of oxygen and nitrogen atoms in the stage III recovery of niobium. Defects were introduced mainly by means of cold-rolling. Specimens were prepared from the material A (O + N < 50 ppm), B (O + N ≃ 210 ppm) or C (O + N ≃ 850 ppm). All specimens showed recovery in the temperature range 100 to 200° C; an additional recovery stage was observed in the material C and nitrogen-doped B.

The values of activation energy for A and B were 0.7 eV. The order of reaction was second for A, while it was first for B. For C, activation energy and the reaction order were 1.2 eV and first, respectively. For the additional stage of C, the value of 3.4 eV was obtained, but the reaction was not simple. From these results and other results concerning the change in hardness, irradiation and quenching experiments, the dominant mechanism for recovery was considered. It was believed that point defects, probably the interstitial atoms, played a very important role in the recovery process of A and B, while in C recovery seemed to be due to migration of oxygen atoms.

1. Introduction

After cold-work or irradiation, all body-centred cubic refractory metals seem to recover in the temperature range (0.10 to 0.20)T_m, where T_m is the melting point (in K) of each metal. The reason why this recovery occurs is not adequately clear at present, although a number of investigations have been carried out on this problem.

There have been, roughly speaking, three kinds of views so far about the origin of that recovery. In the early days, investigators were apt to believe that it originates in vacancy migration, as in the case of stage III recovery of face-centred cubic metals [1-4]. In later days, however, there appeared a few investigators who believed that interstitials were responsible because they can migrate in the temperature range mentioned above [5-7].

Recent investigations have suggested that interstitial impurity atoms play a very important role in the recovery process of cold-worked or irradiated body-centred cubic metals [8-11]. However, Perepezko, Murphy, and Johnson have considered other possibilities in their paper on irradiated vanadium [12]. As Venetch, Johnson, and Mukherjee [13] suggested, the process of stage III recovery of bcc refractory metals has not yet been clearly explained.

The author has also a different opinion on cold-worked or irradiated vanadium, which will be published later. Under present circumstances one should make experiments using an ultra-high purity material or clarify exactly the role of interstitial impurity atoms in order to understand the mechanism of stage III recovery of bcc metals.

In this paper, the author has tried to find out the important role of oxygen and nitrogen atoms in the recovery process of cold-worked or irradiated niobium. The recovery of electrical resistivity and hardness was measured for this purpose. In the following sections, after the experimental procedure has been briefly described, the results and discussion are shown in section 3. Conclusions will be given in section 4.

2. Experimental Procedure

The experiments were carried out on poly-

*Present address: Graphite Research Laboratory, Japan Atomic Energy Research Institute, Tokai-mura, Ibaraki-ken, Japan.

crystalline niobium. The starting materials were electron-beam-melted ingot which was fabricated into plate about 0.1 mm thick, commercial niobium plates 1 mm thick and wires 0.5 mm in diameter.

The fabrication of the ingot was performed by swaging and rolling with or without intermediate thermal treatments. The commercial plates were annealed *in vacuo* (2×10^{-6} torr) at 1300°C and cold-rolled into sheet of about 0.1 mm. In order to obtain the required degree of coldwork, an appropriate number of annealing treatments have been done. Materials used and chemical analysis of them are shown in table I. In this table, the material B-1 and B-2 were made by doping oxygen or nitrogen into the material B.

TABLE I Gas impurity contents of materials used in the experiments and the method of introducing defects.

Material	Impurity content (ppm by weight) O	N	C	H	Form	Defects introduction
A	40	8	80	*	Plate	Forging and rolling
B	200	12	87	*	Plate	Rolling
B-1	1500	28	87	3.6	Plate	Rolling
B-2	2000	60	†	1.9	Plate	Rolling
C	800	40	88	10	Plate	Rolling
D	Nearly the same as C				Wire	Tension

*The values are unknown, but possibly almost the same as those of B-1 or B-2.
†The value is unknown, but possibly almost the same as that of B-1 or B-2.

All the samples, except those fabricated from the material A, were annealed in a vacuum of 2×10^{-6} torr to achieve a standard state. The annealing temperature and time were 1300°C and 2 h, respectively.

The introduction of defects by coldwork was mainly performed by rolling the sample at room temperature, but in some cases samples were deformed by tension. Electrical resistivity was measured at liquid nitrogen temperature with standard dc potentiometric technique. Vickers hardness was also measured at room temperature Recovery anneals were carried out in a silicone oil bath up to about 350°C.

3. Results and Discussion

3.1. Isochronal Annealing Curves

Figs. 1 and 2 show some of the isochronal annealing curves for the samples which were cold-rolled to various degrees. In fig. 1, we can see curves for zone-refined specimens (the materials A and B) and in fig. 2, those for specimens fabricated from commercial metal (the material C).

In both figures the electrical resistance decreases in the annealing temperature range between 100 and 200°C. However, in the case of the commercial metal, which was heavily cold-worked, another recovery stage can be seen at around 270°C, as in the case of vanadium and tantalum [11]. The amount of resistivity change at this additional stage is much smaller than at the main stage. It is also shown in the figure that the specimen cold-worked lightly

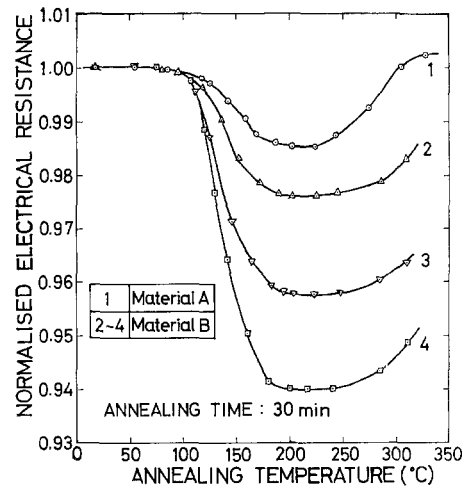

Figure 1 Isochronal annealing curves for cold-rolled niobium. The degrees of cold-work are 15, 90 and 92% for the curve 2, 3 and 4, respectively. Material A was forged and rolled without intermediate annealing treatments.

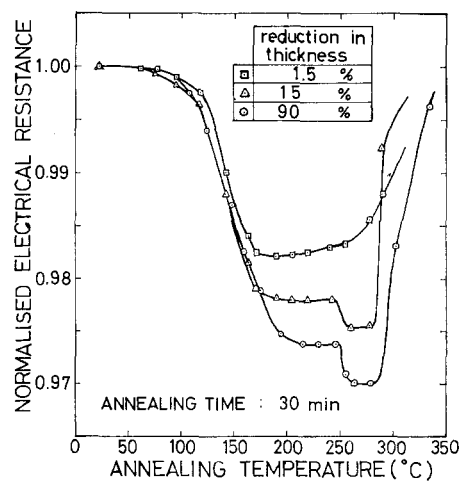

Figure 2 Isochronal annealing curves for cold-rolled niobium (material C).

does not show any recovery in this temperature range.

Fig. 3 shows the similar curves for the specimens fabricated from materials B-1 and B-2. For comparison, curves for the specimens fabricated from the materials B and C are also shown in the figure. It can presumably be said, from this result, that the second stage must be related to the presence of nitrogen, because only the nitrogen-doped specimen, and those fabricated from the material C whose nitrogen content is fairly large, have shown this recovery. The possibility that this recovery stage has appeared because of the presence of carbon may be discarded because the possibility of contamination by carbon during the doping treatment is very small. The results of chemical analysis shown in table I support this view. If contamination by carbon should occur, recovery due to carbon must appear in a higher temperature range [10]. It would be, however, possible that a complex which consists of nitrogen and carbon or oxygen contributes to the recovery stage.

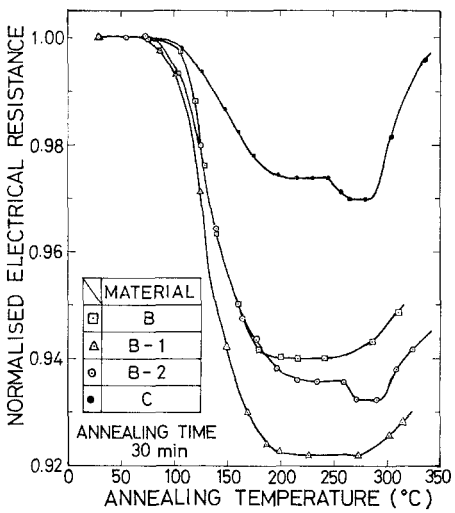

Figure 3 Isochronal annealing curves for cold-rolled specimens prepared from the material B, B-1, B-2 and C. B-1 and B-2 were fabricated from material B by doping with oxygen and nitrogen, respectively. Reduction in thickness of each specimen is as follows: B, 92%; B-1, 89%; B-2, 86%; C, 90%.

It may easily be understood that oxygen atoms affect the first recovery stage, if we compare the curve B with B-1 in fig. 3. Because of the increase of oxygen content, the amount of recovery of electrical resistance has increased about 2% (0.1 $\mu\Omega$-cm). Since the increase of resistivity is 3.9×10^{-3} $\mu\Omega$-cm when 1 ppm by weight of oxygen atoms are dissolved in niobium [14], and the decrease due to trapping by dislocations may be considered to be one-quarter of this value, i.e. about 1×10^{-3} $\mu\Omega$-cm/ppm oxygen [15], a decrease of electrical resistivity of 0.1 $\mu\Omega$-cm would correspond to an oxygen content of about 100 ppm, if the recovery takes place by migration of oxygen towards dislocations and trapping by them. Considering the oxygen content of specimen B-1, this value is reasonable for us to believe that oxygen atoms precipitate at dislocations, at least when the purity of specimen is low.

On the other hand, the resistivity change at the second stage is very small compared with that at the first stage, i.e. $\Delta\rho \sim 0.010\,\mu\Omega$-cm. If we assume that the amount of resistivity change due to precipitation of nitrogen to dislocations is nearly equal to that in the case of oxygen, the changes in the second stage can be considered to appear when about 10 ppm of nitrogen atoms migrate towards dislocations where they precipitate from the matrix. This value seems to be reasonable for the nitrogen migration mechanism mentioned above, but there remain three possibilities that nitrogen atoms may not be migrating towards dislocations by such a simple mechanism. If the amount of resistivity change due to precipitation of 1 ppm nitrogen should be substantially larger than that assumed above, the second stage may originate in precipitation of only 2 or 3 ppm nitrogen. In this case, the value (2 or 3 ppm) must be considered to be rather too small. Thus the following three possibilities are open to be clarified:

(1) Deficiency of sites for precipitation of nitrogen. The fact that the lightly cold-rolled specimen did not show the second recovery stage leads us to consider that the number of sites available for precipitation of nitrogen is a very important factor in the second stage.

(2) Precipitation of N-O cluster which has not so much contribution to resistivity change as an isolated nitrogen atom.

(3) Replacement of the oxygen by nitrogen atoms.

The curve 1 in fig. 2 which represents the recovery of a lightly cold-worked specimen suggests that the first possibility is most probable, but the other curves in the same figure are not inconsistent with the second and third possibilities.

3.2. Isothermal Annealing Curves

Figs. 4, 5 and 6 show some of the isothermal

annealing curves obtained in the experiments. Activation energy and order of reaction were evaluated from these data.

The values of activation energy obtained on the assumption that recoveries occur in a single activated process are summarised in table II, where methods of evaluation are also shown. Fig. 7 shows the t versus $1/T$ plots of heavily cold-worked material A.

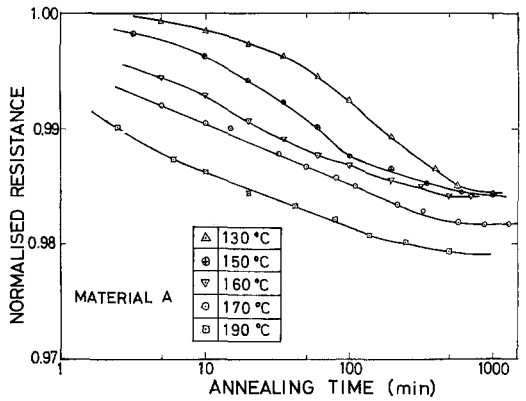

Figure 4 Isothermal annealing curves for the material A, forged and rolled.

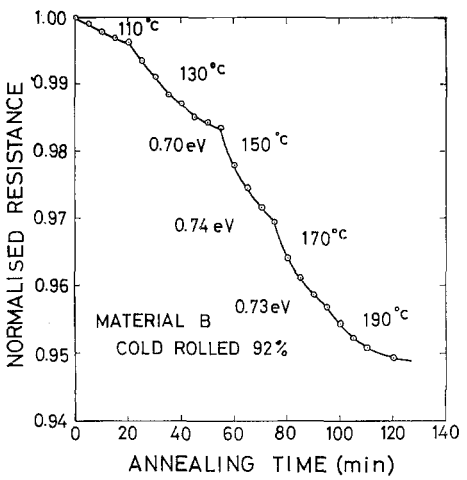

Figure 5 Slope-changes on isothermal annealing at different temperatures in the material B, cold-rolled 92%.

Let us assume that the recovery process proceeds according to the equation

$$\frac{dR}{dt} = -f(R)\exp - \left(\frac{E}{kT}\right), \qquad (1)$$

where R = resistivity, t = annealing time, E = activation energy, k = Boltzmann constant, and

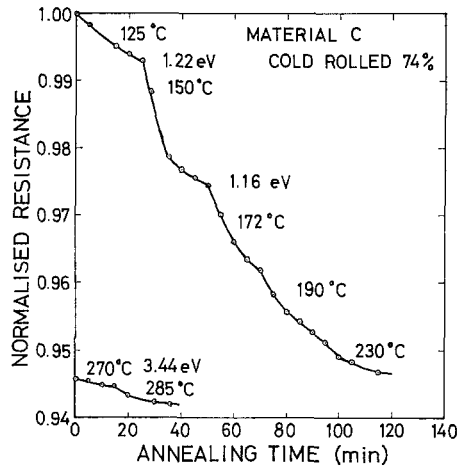

Figure 6 Slope-changes on isothermal annealing a different temperatures in the material C, cold-rolled 74%

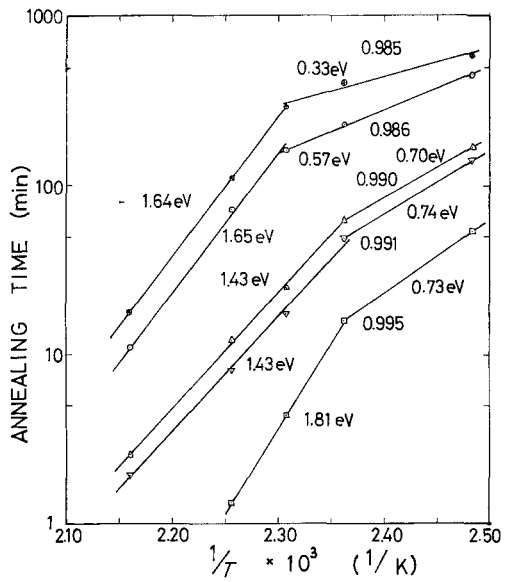

Figure 7 Plots of log time versus reciprocal of the absolute temperature of annealing for the material A, forged and rolled.

T = annealing temperature in K and that the concentration of defects which contribute to recovery is proportional to the amount of electrical resistivity change, i.e.

$$\frac{C}{C_0} = \frac{R - R_f}{R_i - R_f}. \qquad (2)$$

In equation 2, R_i, R_f are the initial resistivity and the final one, respectively. C_0 represents the initial concentration of defects and C is

TABLE II Activation energy for recovery of several cold-rolled specimens.

Material	Reduction in thickness (%)	Method of evaluation	Temperature range (°C)	Activation energy (eV)
A	95	Cross-cut	100–160	0.72
			160–200	1.53
B	92	Ratio of slope	130–150	0.70
			150–170	0.74
			170–190	0.73
C	90	Ratio of slope	131–156	1.25
			156–175	1.27
	74	Ratio of slope	125–150	1.22
			150–172	1.16
			270–287	3.44
B-2	86	Ratio of slope	130–151	1.02
			151–171	0.72
			171–190	1.23
			190–230	1.25
			270–285	3.42

the defect concentration when resistivity is R. From equations 1 and 2,

$$\frac{dC}{dt} = -g(C)\, C_i \exp\left(-\frac{E}{kT}\right). \quad (3)$$

Therefore, if the reaction order is first, i.e. $g(C) \propto C$,

$$\log \frac{C}{C_0} = K_1 t, \quad (4)$$

and if it is second, i.e. $f(C) \propto C^2$,

$$\frac{C_0}{C} = K_2 t + 1. \quad (5)$$

K_1 and K_2 are constant in these equations.

Fig. 8a and b show the (C_0/C) versus t plots of several specimens fabricated from the material A, which were annealed isothermally at various temperatures. The reaction order of this process is second below 160°C, except at the early stage where the so-called $\sqrt{t}$-law seems to be obeyed. Plots of 170 and 190°C annealing followed the $\sqrt{t}$-law, but they gradually showed deviation later. The results obtained from annealing below 160°C are very similar to those of Nihoul and Stals [7], except that the activation energy differs considerably. Recently, Szkopiak and Pouzet [16] have obtained the activation of 1.16 eV for recovery of cold-worked niobium. Soo [17] studied the strain-ageing of niobium to find out a stage governed by activation energy of 0.63 or 0.69 eV preceding the normal oxygen-induced one. The value obtained for the recovery of the material A below 160°C is nearly equal to that in the case of the experiments by Soo. Nihoul and Stals have proposed the mechanism for stage III recovery of cold-worked niobium that intrinsic interstitials migrate and vacancy-interstitial annihilation occurs. However, the author believes that in the experiments of Nihoul *et al* an oxygen migration mechanism, whose reaction can be of second order, is probably dominant, because migration energy of oxygen in niobium is about 1.2 eV, which is just equal to what they observed. Though it is difficult to propose a definite mechanism mentioned above, formation of an oxygen-point defect or oxygen-impurity cluster may be considered. It should also be noted that the chemical analysis of ingot is not always identical to that of the specimen. In the present case, one of the mechanisms which can be proposed may be that a certain kind of point defect migrates towards an interstitial impurity atom or other point defect and annihilates or is trapped by the impurity or defect.

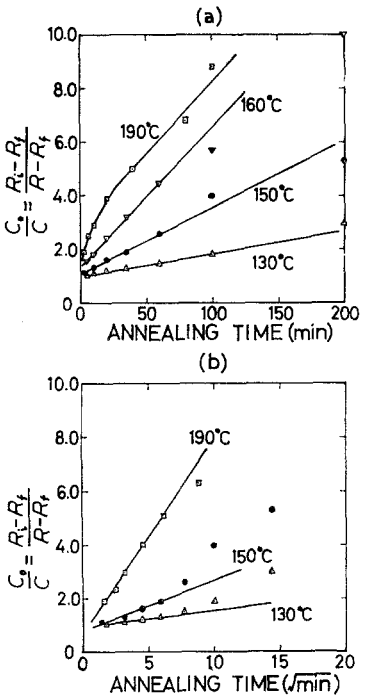

Figure 8 Isothermal recovery of the material A presented in (a) (C_0/C) versus t and (b) (C_0/C) versus $\sqrt{t}$.

After Schultz [5], there may be a few phenomena which are considered to obey the $\sqrt{t}$-law approximately, that is, (1) migration of defect or impurity to grain boundary, (2) migration of

vacancy to dislocation when one takes account of the interaction between vacancy and dislocation and (3) the early stage of vacancy-interstitial annihilation. Among these possibilities, the third one is not probably appropriate as a mechanism by which the recovery above 160°C occurs. It can be considered that the reaction must become second-order as the recovery proceeds, if such annihilation should take place. The second possibility is most probable because the migration energy of vacancy becomes lowered when the interaction is taken in account. In this case, it is likely that migration energy of a vacancy of 2.2 eV, which is the value evaluated by Nihoul and Stals [7], may change to about 1.5 eV. It is believed that vacancies migrate towards dislocations if the concentration of isolated impurity interstitials is low and if the interaction energy between vacancies and impurity atoms is low. However, the first assumption cannot, of course, be discarded. For example, the migration energy of oxygen will be about 1.5 eV, on the assumption that the binding energy of the O-O bond in the oxygen cluster is 0.2 eV or so and an oxygen atom can migrate towards a grain boundary only when the O-O bond is dissociated [18, 19].

Köthe and Schlät also referred to a change in slope of recovery curve for tantalum [20]. According to their experiments, it was observed at 130°C, which became more pronounced at larger degree of deformation. Such a change in slope can be clearly observed in fig. 7, where t versus $1/T$ plots obtained from the recovery curves for the material A in fig. 4 are shown. It should be noted that all the curves shown in fig. 4 are also those for the specimens which were heavily cold-rolled.

Fig. 9a and b show similar plots for specimens fabricated from the materials B and C, respectively. In fig. 9a, the specimens show first-order kinetics. Therefore, the dominant mechanism for this recovery may be that a certain kind of point defect, for example an interstitial atom, migrates towards sinks such as dislocations. The first-order reaction is possibly obtained if a vacancy is trapped by an impurity atom – that is, the interstitial atom cannot annihilate through interaction with vacancy. This may be realised, because the content of interstitial impurity is fairly large in these cases. From the results in fig. 9b, it can be concluded that the first recovery stage of the material C

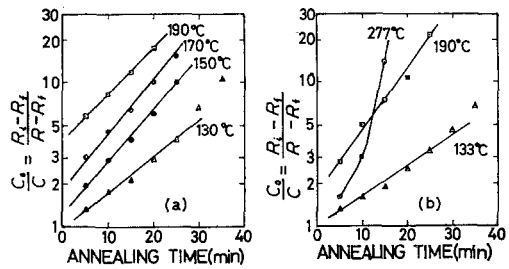

(a) (b)

Figure 9 Isothermal recovery of (a) the material B and (b) the material C, presented in $\log(C_0/C)$ versus annealing time.

is caused by migration of oxygen to dislocations, if one considers the activation energy obtained. The reaction order of the second stage, where the activation energy is very large, appears to be complicated. Therefore, it is likely that this process occurs due to migration or replacement of a defect-impurity complex.

3.3. Concentration of Defects and Oxygen

The resistivity change shown in fig. 1 is about $0.15\mu\Omega$-cm in the case of the 90% cold-rolled specimen fabricated from the material B. The similar value for the specimen fabricated from the material C is about $0.11\mu\Omega$-cm. It is, however, about $0.04\mu\Omega$-cm for the specimen 1 shown in fig. 1, which was prepared from the material A.

Since the resistivity change due to precipitation of oxygen at dislocation is about 1×10^{-3} $\mu\Omega$-cm/ppm oxygen, the values evaluated above may correspond to 150 (material B), 110 (material C), and 40 (material A) ppm oxygen, if the oxygen atom should migrate towards a dislocation and precipitate there. In the case of the material C, it should be believed that oxygen atoms of 110 ppm can precipiate, but in the other cases, the values calculated above are considered to be, at least, fairly large, if one compares this value with the chemical analysis. For it is considered that all the present oxygen atoms in a specimen cannot contribute to the resistivity change. There may be a lot of oxygen atoms which have already locked the dislocation or formed the cluster (pair, triplet etc.).

If the resistivity change which results from the annihilation of vacancy with interstitial or formation of point defect-impurity pairs of 1 at. % is $10\mu\Omega$-cm/%, it is required that the fraction of pairs must be 4×10^{-5} for A and 1.5×10^{-4} for B, in order to explain the change

of resistivity associated with the recoveries. These values are rather reasonable, when one considers that the specimens were heavily cold-worked. Thus, it may be said that the activation energy and reaction order obtained have been reasonably explained.

3.4. Dislocation Density

Assuming that n oxygen atoms can precipitate at one dislocation precipitation site, we obtain the equation

$$C_S = n\left(\frac{\rho_0}{a}\right)\left(\frac{1}{a^3}\right) = na^2\rho_0\,, \qquad (6)$$

where C_S, ρ_0 and a are the saturated concentration of oxygen precipitating at dislocations, density of dislocations and lattice constant, respectively.

Since the number of jumps j is obtained from the experimental results, ρ_0 can be evaluated. When T, t are the isothermal annealing temperature and time, respectively, the required number of jumps of oxygen to dislocation is given by

$$j = t\nu Z\exp\left(-\frac{E}{kT}\right), \qquad (7)$$

where ν, Z, k, E are atomic frequency ($\simeq 10^{13}$/sec), co-ordination number ($Z = 8$), Boltzmann constant and activation energy for recovery, respectively.

If we assume that oxygen atoms migrate towards dislocations randomly, and the distance of migration of oxygen is nearly equal to the mean distance between dislocations,

$$j = \frac{1}{a^2\rho_0}\,. \qquad (8)$$

Considering that 100 ppm oxygen atoms may precipitate, $C_S \simeq 1.2 \times 10^{-4}$ and $\rho_0 \simeq 1.4 \times 10^{11}$, if we choose the values of a and n as 2.9×10^{-8} cm and 5, respectively. Here, the value of n was chosen according to Narutani [21], who had obtained it by evaluating the decrease of the oxygen Snoek peak and the dislocation density of vanadium. This value of ρ_0 is believed to be reasonable for heavily cold-worked metal.

In table III, ρ_0's calculated from equations 7 and 8 are summarised for several specimens. In the case of the material C, ρ_0's are consistent with the value of ρ_0 which has been obtained from equation 6. The fact that the ρ_0's in the table are rather larger than those obtained from equation 6 is believed to result from the neglect of the oxygen atom which has already locked the dislocation. Thus, it must be emphasised that the precipitation of oxygen to dislocations occurs in the recovery process of cold-rolled material C. However, the situation is entirely different from that mentioned above in the cases of the materials A and B. Therefore, it may be believed in the latter cases that the oxygen migration to dislocation is not the dominant mechanism.

TABLE III Dislocation density calculated from the half decay time.

(1) Material A cold-rolled 95%

Annealing temperature (°C)	Half decay time (sec)	Number of jumps	Dislocation density (1/cm²)	Activation energy (eV)
130	6600	5.3×10^{8}	2.3×10^{7}	0.72
150	2100	4.7×10^{8}	2.6×10^{7}	0.72
160	780	2.6×10^{8}	4.6×10^{7}	0.72
170	1170	7.0×10^{-1}	1.3×10^{15}	1.5
190	210	2.9×10^{-1}	4.1×10^{15}	1.5

(2) Material C cold-rolled 80 or 90%

Annealing temperature (°C)	Half decay time (sec)	Number of jumps	Dislocation density (1/cm²)	Activation energy (eV)
156*	1020	1.0×10^{2}	1.1×10^{12}	1.25
190*	300	2.2×10^{3}	5.1×10^{11}	1.25
175†	480	1.3×10^{3}	8.6×10^{11}	1.25

*Cold-rolled 80%. †Cold-rolled 90%.

The calculated values for material B cold-rolled about 90% are the same as those for the lower-temperature recovery of material A in order.

3.5. Quenching Experiments and the Measurement of Hardness

Fig. 10 shows the ageing curve for the specimens which were thermally treated at 350°C for 180 min. after cold-work and water-quenched. Specimen B-1 has no peak at 250°C, while the curve for specimen C shows the peak. From this result, it is considered that the replacement of oxygen occurs really above 250°C in the latter case. The increase of resistivity above 300°C has been considered to originate in the decomposition of oxygen cluster or the de-trapping of oxygen from dislocations. Assuming this, activation energy of decomposition or de-trapping became 1.65 eV in the present case. It is believed that the replacement occurs with activation energy equal to the value evaluated by means of the equation,

$$E \simeq E_N - T_N + E_0 + D_0 \qquad (9)$$

where E_N, T_N, E_0, D_0 are the migration energy of nitrogen, energy decrease due to precipitation of nitrogen to dislocations, migration energy of oxygen and de-trapping energy of oxygen from dislocations, respectively. This value of E will be nearly equal to the activation energy of the second recovery stage, if one chooses the value of E_N and E_0 as 1.65 and 1.20 eV, respectively, and assumes that $D_0 - T_N = 0.5 \sim 0.6$ eV, i.e. $T_N \simeq 1.1$ eV. The isothermal ageing curve for the specimen prepared from the material C, which was thermally treated at 330°C in 200 min. after cold-work (74%) cold-rolling), is shown in fig. 11. The curves for the material B and B-1 were also obtained. However, they are not shown, because they have shown almost the same features as those in fig. 11. It is difficult to analyse the very complicated curve shown in fig. 11. However, it can be explained as follows. The oxygen atom precipitates on dislocations by ageing treatments, but at higher temperatures, clusters whose diameter is small become unstable. A lower limit of diameter of the cluster which is stable at a certain ageing temperature exists. As the temperature increases, so does this lower limit. Therefore, the unstable cluster decomposes in a few minutes after the temperature has increased, and the resistivity increases. The subsequent decrease is believed to result from the precipitation to dislocation and the formation of the cluster which is larger in diameter. Above 300°C, the decomposition of the cluster and de-trapping of oxygen from dislocations must make the resistivity increase.

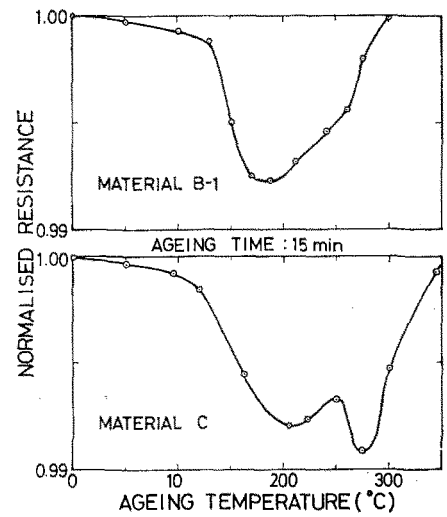

Figure 10 Ageing curves for the materials (a) B-1 cold-rolled 89% and (b) C cold-rolled 90%, which were thermally treated at 350°C for 180 min after cold-work and quenched into water.

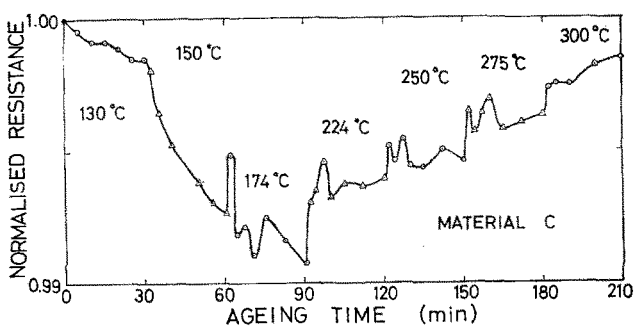

Figure 11 Ageing curves at various temperatures for the material C cold-rolled 74%, which was thermally treated at 330°C for 220 min after cold-work and quenched into water.

The analysis of the measurements of hardness is also difficult. Differences between the materials B and C, however, were observed in the annealing curves. For example, some of the isothermal annealing curves are shown in figs. 12 and 13. The increase of hardness is commonly observed in the early stage of recovery of the material C. This suggests the important effect of impurity interstitial in material C, while the decrease observed in the case of the material B is believed to correspond to annihilation of point defects. The situation was almost the same with regard to isochronal annealing curves.

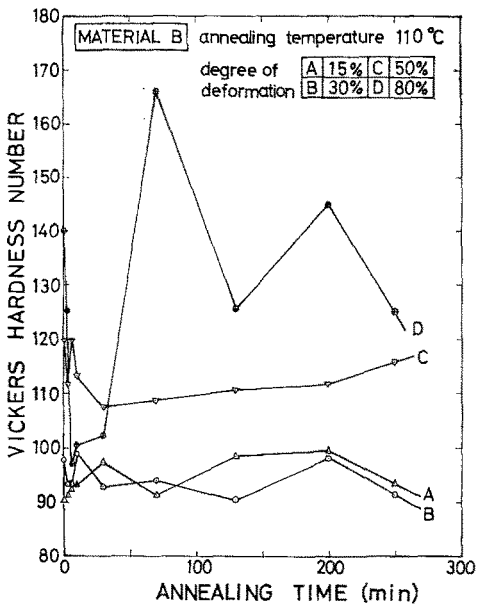

Figure 12 Isothermal annealing curves for the specimens fabricated from the material B, which were cold-rolled to various degrees of deformation.

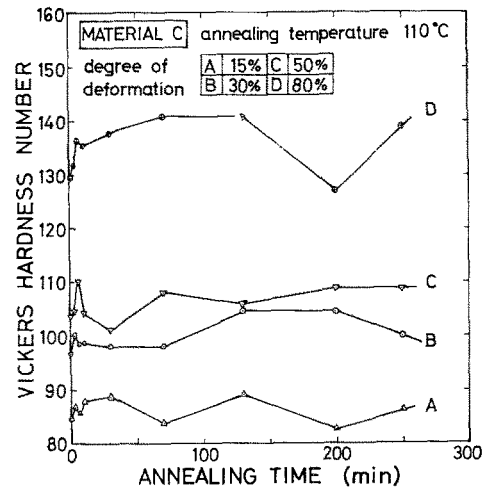

Figure 13 Isothermal annealing curves for the specimens fabricated from the material C, which were cold-rolled to various degrees of deformation.

3.6. The Increase of Resistivity due to Cold-Work and the Irradiation Experiments

Fig. 14 shows the resistivity change due to cold-work (elongation) and the subsequent decrease which results from the annealing at 200°C for 30 min. By these annealing treatments, the resistivity decreases and becomes lower than the value before cold-work, though it is not the case for a specimen which is cold-worked lightly. This fact also suggests that the precipitation to dislocations occurs.

The results of irradiation experiments show that the specimens irradiated by fast neutrons do not recover in the temperature range where so-called stage III recovery is observed. This situation is shown in fig. 15. Therefore, it appears that the dislocations do play a very important role in the recovery of niobium, though the origin of the reverse-annealing in the figure is not clear at present.

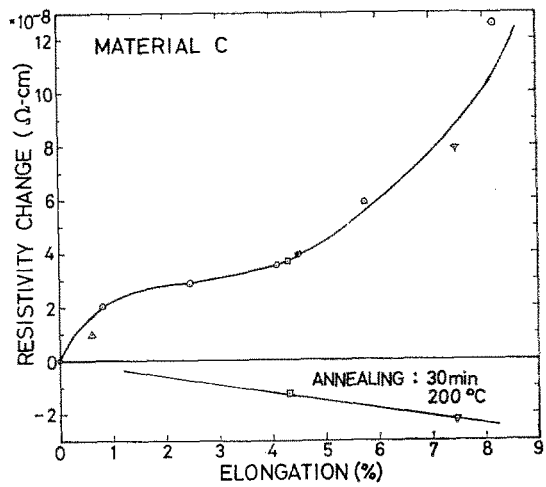

Figure 14 Resistivity increase due to cold-work by tension and the subsequent decrease due to annealing at 200° C for 30 min.

4. Conclusions

The author has shown that the characteristics of so-called stage III recovery of niobium is dependent on the oxygen and nitrogen contents. In order to find out the differences which originate from different methods of introducing defects,

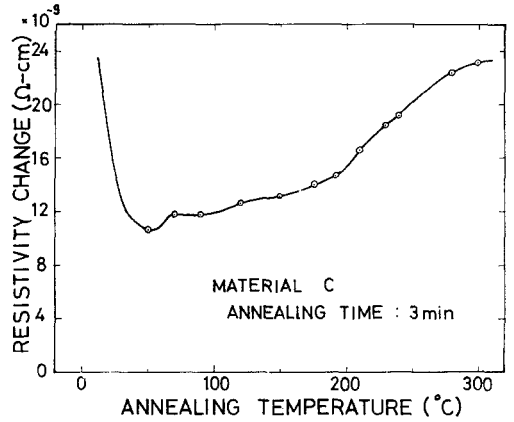

Figure 15 Isochronal annealing curve for the material C irradiated by fast neutrons ($E \geq 1$ MeV, 2×10^{16}/cm^2). The specimen was irradiated at liquid-helium temperature and the annealing curve was obtained from liquid nitrogen temperature to 300°C. Here, the curve above room temperature is shown.

cold-worked or irradiated specimens are examined, though the studies of the latter were not sufficiently extensive.

Conclusions derived are as follows. The recovery of high purity specimen results from vacancy-interstitial annihilation and/or interstitial-impurity pair formation below 160°C. As for recovery above 160°C, several possibilities can be considered. For example, mechanisms such as vacancy migration to dislocations or oxygen migration to a grain boundary has been proposed.

In the material of ordinary purity, the dominant mechanism is that the point defect (probably the interstitial atom) migrates to sinks such as dislocations and impurity atoms.

Commercial metal of low purity has shown two-stage recovery. The first stage originates in the migration of oxygen to dislocations, because the activation energy is equal to the migration energy of oxygen, and the reaction is first-order. It can be accepted in the present experiments that the second stage results from the replacement of a nitrogen atom with an oxygen atom at the precipitation site of dislocations.

Since irradiated specimens have not shown stage III recovery, the existence of dislocation is believed to be indispensable for the recovery of ordinary or low-purity niobium. The fact that the magnitude of resistivity decrease is larger than that of increase due to cold-work in the case of the low-purity material suggests that interstitial impurity atoms affects the recovery behaviour considerably.

Acknowledgements

The author wishes to thank Professor Y. Mishima and Dr S. Ishino for their helpful instruction and guidance throughout this work. He is indebted to Dr S. Okuda for permission to use the facilities at JAERI and for valuable discussions, and to Mr Y. Arai for technical assistance.

References

1. D. G. MARTIN, *Acta Metallurgica* **5** (1957) 371.
2. M. J. MAKIN and F. J. MINTER, *ibid* **7** (1959) 361.
3. L. A. NEIMARK and R. A. SWALIN, *Trans. AIME* **218** (1960) 82.
4. D. E. PEACOCK and A. A. JOHNSON, *Phil. Mag.* **8** (1963) 563.
5. H. SCHULTZ, *Acta Metallurgica* **12** (1964) 649.
6. J. NIHOUL, *Phil. Mag.* **9** (1964) 167.
7. J. NIHOUL and L. STALS, *Phys. Stat. Sol.* **8** (1965) 785.
8. A. R. ROSENFIELD, *Acta Metallurgica* **12** (1964) 119.
9. L. J. CUDDY and J. C. RALEY, *ibid* **14** (1966) 440.
10. J. M. WILLIAMS, J. T. STANLEY, and W. E. BRUNDAGE, USAEC Report, ORNL-4097 (1967).
11. A. KÖTHE and F. SCHLÄT, *J. Mater. Sci.* **2** (1967) 201.
12. J. H. PEREPEZKO, R. F. MURPHY, and A. A. JOHNSON, *Phil. Mag.* **19** (1969) 1.
13. J. VENETCH, A. A. JOHNSON, and K. MUKHERJEE, *J. Nucl. Mat.* **34** (1970) 343.
14. C. S. TEDMAN, JUN., R. M. ROSE, and J. WULFF, *Trans. Met. Sol. AIME* **230** (1964) 1732.
15. M. ETO and T. NARUTANI, to be published.
16. Z. C. SZKOPIAK and B. POUZET, Jül-Conf-2 II (1968) 709.
17. P. SOO, *Phys. Stat. Sol.* **32** (1969) 815.
18. R. GIBARA and C. A. WERT, *Trans. Met. Sol. AIME* **236** (1966) 924.
19. R. GIBARA and C. A. WERT, *Acta Metallurgica* **14** (1966) 1095.
20. A. KÖTHE and F. SCHLÄT, *Phys. Stat. Sol.* **21** (1967) K73.
21. T. NARUTANI, private communication.

Received 23 August and accepted 3 December 1971.